fire

MDPI

Article

Multiparameter Detection of Summer Open Fire Emissions: The Case Study of GAW Regional Observatory of Lamezia Terme (Southern Italy)

Luana Malacaria [1,*], Domenico Parise [1], Teresa Lo Feudo [1,*], Elenio Avolio [1], Ivano Ammoscato [1], Daniel Gullì [1], Salvatore Sinopoli [1], Paolo Cristofanelli [2], Mariafrancesca De Pino [1], Francesco D'Amico [1] and Claudia Roberta Calidonna [1]

[1] Institute of Atmospheric Sciences and Climate of National Research Council, Area Industriale Comp. 15, I-88046 Lamezia Terme, CZ, Italy; d.parise@isac.cnr.it (D.P.); elenio.avolio@cnr.it (E.A.); ivano.ammoscato@cnr.it (I.A.); daniel.gulli@cnr.it (D.G.); salvatore.sinopoli@cnr.it (S.S.); mariafrancesca.depino@cnr.it (M.D.P.); f.damico@isac.cnr.it (F.D.); claudiaroberta.calidonna@cnr.it (C.R.C.)

[2] Institute of Atmospheric Sciences and Climate of National Research Council, Via P. Gobetti 101, I-40129 Bologna, BO, Italy; paolo.cristofanelli@cnr.it

* Correspondence: l.malacaria@isac.cnr.it (L.M.); teresa.lofeudo@cnr.it (T.L.F.)

Abstract: In Southern Mediterranean regions, the issue of summer fires related to agriculture practices is a periodic recurrence. It implies a significant increase in carbon dioxide (CO_2) emissions and other combustion-related gaseous and particles compounds emitted into the atmosphere with potential impacts on air quality and global climate. In this work, we performed an analysis of summer fire events that occurred on August 2021. Measurements were carried out at the permanent World Meteorological Organization (WMO)/Global Atmosphere Watch (GAW) station of Lamezia Terme (Code: LMT) in Calabria, Southern Italy. The observatory is equipped with greenhouse gases and black carbon analyzers, an atmospheric particulate impactor system, and a meteo-station for atmospheric parameters to characterize atmospheric mechanisms and transport for land and sea breezes occurrences. High mole fractions of carbon monoxide (CO) and carbon dioxide (CO_2) coming from quadrants of inland areas were correlated with fire counts detected via the MODIS satellite (GFED-Global Fire Emissions Database) at 1 km of spatial resolution. In comparison with the typical summer values, higher CO and CO_2 were observed in August 2021. Furthermore, the growth in CO concentration values in the tropospheric column was also highlighted by the analyses of the L2 products of the Copernicus SP5 satellite. Wind fields were reconstructed via a Weather Research and Forecasting (WRF) output, the latter suggesting a possible contribution from open fire events observed at the inland region near the observatory. So far, there have been no documented estimates of the effect of prescribed burning on carbon emissions in this region. This study suggested that data collected at the LMT station can be useful in recognizing and consequently quantifying emission sources related to open fires.

Keywords: open fire; climate change; atmospheric greenhouse gases; black carbon emission; Mediterranean basin

Citation: Malacaria, L.; Parise, D.; Lo Feudo, T.; Avolio, E.; Ammoscato, I.; Gullì, D.; Sinopoli, S.; Cristofanelli, P.; De Pino, M.; D'Amico, F.; et al. Multiparameter Detection of Summer Open Fire Emissions: The Case Study of GAW Regional Observatory of Lamezia Terme (Southern Italy). *Fire* **2024**, *7*, 198. https://doi.org/10.3390/fire7060198

Academic Editors: João Neves Silva and Duarte Oom

Received: 30 May 2024
Revised: 10 June 2024
Accepted: 10 June 2024
Published: 14 June 2024

1. Introduction

Forest fires constitute a major socioeconomic, human safety and environmental hazard in the Mediterranean. The main dynamics influencing forest fire potential are climate and weather. These factors together with vegetation composition and conditions, and chiefly human activities, play an essential role in fire regimes [1]. Fire events influence many relevant ecosystem processes and patterns, including the carbon cycle, vegetation structure, and climate at regional and global scales [2]. Fire events have been considered a decisive factor in the Mediterranean environment that historically shaped ecosystems and drove

several plant adaptations [3–5]. The contribution of extreme winds with extreme drought and/or heatwaves has been identified as a crucial factor for preconditions of wildfire occurrence [6], in conjunction with specific atmospheric conditions which have persisted on Earth for several hundred million years [7].

Under changing climatic conditions, the danger of future fires and the frequency of fires, as well as the extent of large wildfires are all expected to increase throughout the Mediterranean basin [6,8,9]. Regional droughts attributable to climate change and temperature increases, plus the build-up of available fuels, have increased fire hazards [10,11]. The examination of real fire events is essential to learn from past incidents about fire spread mechanisms [12], combustion products [13–19], firefighting activities, home survivability, and socio-economic impacts. At the beginning of this century, severe forest fires consistently affected European Mediterranean countries such as Italy, Greece, Portugal, France and Spain. These regions on average collectively account for approximately 85% of the total burnt area in Europe per year, according to Costa [1]. Significant increases in wildfire outbreaks have occurred in Calabria, a Southern Italian region, during the investigation period, i.e., since 2017 to 2021. Calabria is one the most devoted regions to agriculture in Italy. In detail, the yearly amounts of crop, agro-industry, fruit tree, and livestock rests produced in Calabria have been estimated in terms of waste dry materials [20], which could be possible sources of fire events in the region. During the dry season, the accumulated biomass available for burning becomes highly flammable, and fire can rapidly spread from grasslands to forests. Summer seasons are characterized by high temperatures observed across Southern Italian regions, where agriculture practices favor the occurrence of open fires. Key examples of factors that both regionally and locally outweigh fire weather as controls on fire activity are the presence of human ignitions in regions that are not naturally fire prone, the fragmentation of fire-prone landscapes by agriculture, and weather conditions affecting vegetation growth and fuel build-up. Calabria does not have a history of such large episodes nor a precedent of carrying out detailed post-fire investigations. Prevention program were elaborated in order to disallow extreme fires. The AIB (Anti Incendio Boschivo, Anti-Forest Fire) plans of 2022–2023 [21–23] foresee the capillary activity of territory monitoring integrated by drone deployment to the most exposed areas named "zero–tolerance campaign". The communication campaign of the zero-tolerance plan was extensively carried out by main media and social media through daily information campaigns. Nevertheless, despite this prevention approach in trying to limit fire events through a risk plan, there is still a paucity of relevant data to investigate the relative influences of the factors known to affect fire spread, human subsistence, and home and vegetation survivability. This framework presents a synergy between the experimental, satellite and modeling results, the methodology applied to identify fire sources and fire spreading mechanisms, and the consequent discussion of the results. In this work, we focus on the regional impact of fire events on the atmospheric composition in Southern Italy. The measurements of atmospheric parameters are performed at the regional World Meteorological Organization/Global Atmosphere Watch (WMO/GAW), a station operated by the ISAC-CNR (National Research CouncilInstitute of Atmospheric Sciences and Climate) at Lamezia Terme (LMT, 38.88 N, 16.23 E; 6 m *above sea level*). In particular, for the period 2017–2021, we considered atmospheric observations of equivalent black carbon (eBC), CO and CO_2, in correlation with the direction and speed of the local wind fields. eBC is a component of incomplete combustion by products commonly referred to as soot and causes major environmental issues [24–26]. Recently, model results and field measurements have shown that aerosols may have important climatic impacts [13]. CO_2 is the most important greenhouse gas directly affected by anthropogenic emissions (WMO, 2023 https://library.wmo.int/idurl/4/68532 accessed on 26 March 2024), while CO is an effective tracer of combustion processes [27].

Specific analyses were carried out to investigate the possible correlation between the occurrence of elevated eBC, CO and CO_2 values with the presence of open vegetation fires. A statistical analysis was conducted to identify the burnt sites and the frequency of fire

event occurrences. Furthermore, a detailed analysis of open fire events is described to determine the highest pollutant values in relation to ground fire occurrence together with air masses circulation. For this case study, meteorological simulations were considered to underpin the prevalent atmospheric circulation. Atmospheric modeling reconstruction was carried out for a more comprehensive analysis. In this study, we took into account the temporal window between 8 and 12 August 2021, where a series of consecutive fires occurred in areas close to the measurement site, in order to detect the presence of products of forest fires and wildfire plumes. Detailed analysis was carried out considering both surface and column tropospheric properties. For this purpose, we collected data from several instruments and satellite products. In the period of fire events occurrence, the total column of measured CO, using the COPERNICUS constellation SP5 satellite, was also analyzed. The analysis of experimental data corroborated by satellite data and the use of high resolution Weather Research and Forecasting (WRF) model allowed the correlation of aerosol and gaseous species detected at the LMT experimental site, to the fire sources which occurred in the south-southeastern areas with respect to the observatory. This paper is organized as follows: Section 2 describes the Materials and Methods we used; Sections 3 and 4 describe the results and discussion, respectively; and conclusions are drawn, finally.

2. Materials and Methods

In this section, we describe a comprehensive dataset consisting of several instruments, used for our study. Satellite and modeling tools are also described together with the method adopted in order to identify fire events registered in the region near the LMT experimental site. Specific information about the adopted observation techniques is reported in Table 1.

Table 1. Instruments and models used with the information regarding analysis results and temporal resolution of each.

Instruments	Analysis Results—Spatial Resolution	Temporal Resolution
CRDS analyzer, Model G2401, Picarro	CO (ppb), CH_4 (ppb), CO_2 (ppm), H_2O (ppm)	Every 5 s
MAAP, Model 5012, Thermo Scientific	Equivalent Black Carbon, eBC ($\mu g/m^3$)	Every 1 min
SWAM, Model 5a-Dual Channel Monitor, FAI Instrument	PM_{10} and $PM_{2.5}$ ($\mu g/m^3$)	Every 24 h
Weather Transmitter, Model WTX520, Vaisala	Temperature (°C), wind speed (m/s), wind direction (°)	Every 1 min
MODIS-GFED4	The main fire events; count fires 1 km × 1 km	Daily
Weather Research and Forecasting model (WRF) version 4.2, NCAR, NOAA, and AFWA	Temperature (°C), wind speed (m/s), wind direction (°); 2 km × 2 km	Every 3 h
SP5 Copernicus	Tropospheric column of CO (mol/m^2); 3.5 km × 5.5 km	Daily

2.1. The Experimental Site

The CNR-ISAC observatory in Lamezia Terme (CODE: LMT 38.88 N 16.23 E; 6 m *above sea level*) is a Regional WMO/GAW station. LMT is a coastal site located 600 m inland from the Tyrrhenian Sea coastline (Figure 1). The area is characterized by anthropic pollution emissions linked to transportation and agriculture, mainly due to the presence of the nearby A2 highway and the town of Lamezia Terme, both located to the northeast from the observatory. In particular, the highway runs around the observatory location clockwise

from north to south, and crosses the area located 7 km (northward) to 3.5 km (southward) from the observatory. The Lamezia Terme International Airport (IATA: SUF, ICAO: LICA) is located northward with respect to the measurement site.

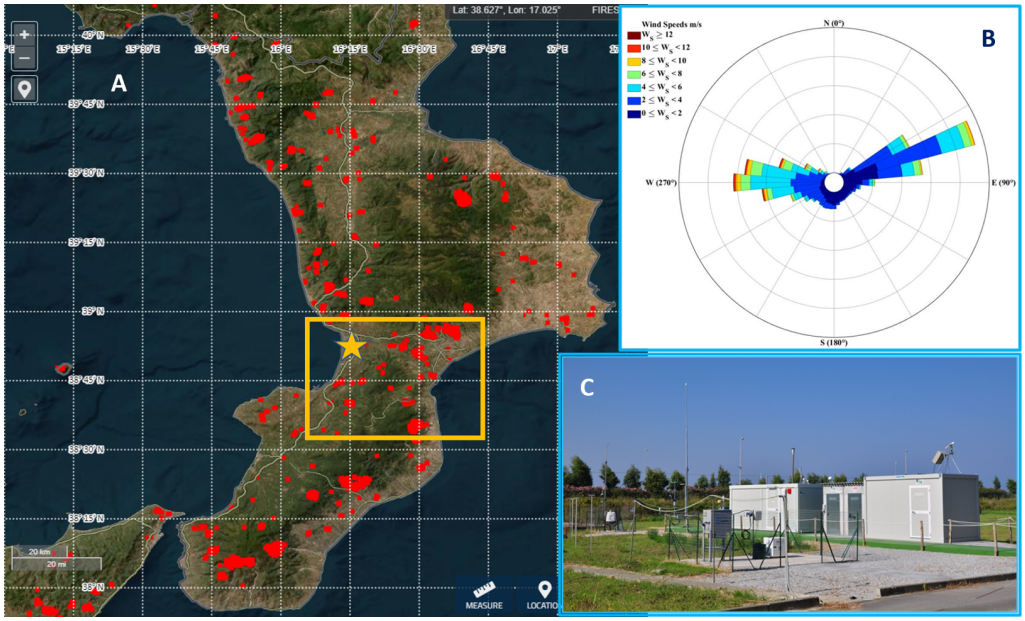

Figure 1. From the left, clockwise: (**A**) the main fire events in Calabria between 8 and 12 August 2021, tracked down from MODIS satellite imaging (red spots), location of the CNR-ISAC WMO/GAW regional site (orange star), Lamezia Terme Observatory and the surrounding area of study (orange box); (**B**) local wind rose centered at LMT–hourly data of wind direction and wind speed for the entire 2017–2021 period; (**C**) LMT Observatory equipment.

Of particular interest is the position of the experimental site within the geodynamic framework of the Calabria–Peloritani Arc, due to its location in the narrowest area within the trough that connects the Ionian and Tyrrhenian seas, which is also the narrowest area in the entire country. The area is characterized by local moderate wind breezes, converging on the Marcellinara gap between the two seas (orange box Figure 1). The sea breeze is well developed during daytime hours, when the wind flows from the west to the east, while the flow is reversed during the night-time period due to land breezes. The predominant synoptic circulation overlap with local breezes preserves a strong directionality from the west (Figure 1) [28,29].

Figure 1 also reports the map showing the main fire events occurred between 8 and 12 August 2021 in Calabria, tracked down from MODIS satellite imaging (red spots).

2.2. The WMO/GAW Site of Lamezia Terme

Several instruments within different monitoring programs have been active at LMT since 2015. The WMO/GAW station is equipped with a cavity ring-down spectroscopy (CRDS) analyzer (Picarro G2401) used to provide simultaneous and precise measurements of carbon monoxide (CO), methane (CH_4), carbon dioxide (CO_2) and water vapor (H_2O).

Patented CRDS technology enables an effective measurement path length of up to 20 km in a compact cavity, which results in high precision and sensitivity in a small-footprint analyzer.

The measurement principle is based on the near-infrared laser absorption technique based on the measure of the rate of exponential decay of light intensity inside the ring-down cavity itself. The three lasers used in the analyzers emit up to 50 mW. From the absorption spectrum of a given gas, it is possible to calculate its mole fraction by measuring the height of the absorption peak, which can be acquired from the rate of light decay. CRDS-based measurements are carried out as per GAW/WMO guidelines and protocols (World Meteo-

rological Organization, 20th WMO/IAEA Meeting on Carbon Dioxide, other Greenhouse gases and related measurement techniques, GGMT-2019) [30]. To sample ambient air, the instrument is connected to a sampling head specifically designed for trace gases. Original raw data are aggregated to hourly mean values. Data are screened to detect anomalous values by inspecting the instrument diagnostics and by considering station logbook for both scheduled and non-scheduled maintenance. A set of three primary standards of calibration from NOAA-GML (National Oceanic and Atmospheric Administration-Global Monitoring Laboratory) is available at LMT: CB10928, CB11039 and CB11164. Furthermore, target gases are used as quality control measures. Routine calibrations are carried out measuring the three NOAA cylinders every two weeks: three injection cycles are implemented with each single injection lasting 30 min. Aerosol particles are sampled with a PM_{10} sampling head equipped with a unique pump having a flow rate of 200 L/min. The aerosol stream is split isokinetically into several instruments such as a Multiangle Absorption Photometer, MAAP 5012 Thermo Scientific [31], and a Beta Attenuation Sampling and Measurement System, FAI SWAM 5a-Dual Channel Monitor.

The SWAM 5a Dual Channel Monitor is a sampling and mass measurement system of airborne particulate material (PM) on filter membranes which allows PM_{10} and $PM_{2.5}$ mass concentration measurements using low volume (2.3 m^3/h). Mass measurement is carried out using an internal β source with nominal activity equal to 3.7 MBq (100 µCi). Thanks to the combination of the β absorption measurement technique with sequential sampling technology and two different sampling heads, the instrument provides, at the end of each operating cycle, mass concentration values of PM_{10} and/or $PM_{2.5}$ depending on the particle size cut of the used head. This instrument operates in successive cycles: the duration of a cycle identifies the duration of sampling on each filter and is programmable by the operator: by default, it is set to 24 h. The accumulation of suspended particulate material occurs for a defined amount of time; the mass evaluation from collected particulate is performed immediately after the sampling period, without any interruptions or downtime. The capacity of the filter loading/unloading containers is 35 filter holders (72 as an option).

The MAAP operates according to WMO/GAW specification [30] to monitor continuous measurements of equivalent black carbon (eBC) concentrations at 637 nm with 1 min resolution time. The sample is drawn into the instrument through the inlet by the internal pump set with a flow rate of 16.7 L/min. The sample is drawn into the instrument through the inlet, flows through the down tube and settles on the glass fiber filter tape. The filter tape will accumulate an aerosol sample towards a threshold value, whereupon the filter tape will automatically advance prior to reaching saturation. Inside the detection chamber, a 670 nm visible light source is directed at the deposited aerosol and filter tape matrix. The light transmitted into the front hemisphere and reflected into the back hemisphere is measured by a series of photo-detectors. During sample accumulation, the light beam is attenuated from an initial reference reading from a clean filter spot. The reduction in light transmission, multiple reflection intensities and air sample volume are continuously integrated over the sample run period to provide a real-time data output of eBC concentration measurements. For more details, see [31]. Meteorological variables such us barometric pressure, temperature, wind speed and direction, accumulated rain (averaged on a 10 min basis) and relative humidity were collected by an automatic weather station (Vaisala WXT520, Finland) at 10 m *above sea level*.

A homogeneous dataset is organized starting from raw data, following the aggregation on a hourly basis for all considered instruments. Quality check and validation statistical methods are applied to raw data in order to filer out outliers and problems likely due to technical issues, while routine calibration methods are normally run. As a result of this filtering process, we report that the percentages of 1.2%, 27% and 2% of all data are rejected respectively for MAAP, Picarro instruments and SWAM datasets collected over the observation period (2017–2021).

2.3. Satellite Products

2.3.1. Fire Location (MODIS–GFED4)

The Global Fire Emission Dataset-Version 4 (GFED4) [32] and online GFED Analysis Tool, https://www.globalfiredata.org/related.html#gfed4, accessed on 9 June 2024, derived by the MODIS (Moderate Resolution Imaging Spectroradiometer) L2 fire products, with 1 km data resolution (at the NADIR) are used to count the daily number of fires that occurred yearly (2017–2021) in the months of August. In particular, with the aim of investigating the possible impact of local crop fires to the atmospheric composition variability observed at LMT, we consider the number of fires that occurred over a region (4112 km^2) representative for local emissions (see Figure 1). The spatial extension of this "focus" region is set to include the valley between the Ionian and the Tyrrhenian Sea, which could favor the transport of air masses across the region.

2.3.2. CO Total Column—Level-2 Data Analysis

Sentinel-5P, a global air pollution monitoring satellite, was launched by the European Space Agency (ESA) on 13 October 2017 as part of the Copernicus mission [33]. The Tropospheric Monitoring Instrument (TROPOMI), which is carried on Sentinel-5P, is in a low-Earth afternoon polar orbit with a swath of 2600 km. It performs daily scans on the whole globe, and it is currently the most advanced atmospheric monitoring spectrometer. Ever since 6 August in 2019, it has performed scans having a spatial resolution of 3.5 km × 5.5 km with a high signal-to-noise ratio; such a resolution is among the finest which are currently available. Operational Level 2 (L2) products are currently available for public access https://dataspace.copernicus.eu/explore-data/data-collections/sentinel-data/sentinel-5p, accessed on 9 June 2024. The daily data are downloaded in netcdf format, and the algorithm reads all the parameters necessary for the processing purposes. The first step is extracting latitude (lat) and longitude (lon) and translating them to along and across track dimensions. Trace gases data are analyzed and divided into arrays meant to be mapped to the region of interest. After excluding values by applying the condition $Qa < 0.5$, we represent the array as a georeferenced map. A feature of the developed algorithm performs a comparison between a specific point of the coordinates (site target) within the area of interest and the satellite measurements near the target. The developed method selects the minimum distance from the target to the slightest distance in the array.

Along with the discussion, the total column observations of CO are presented either in mol/m^2 or in $molecule/cm^2$, using the multiplication factor of 6.02214×10^{19}, suggested by ESA [34]. According to the technical documents, we select TROPOMI L2 pixels with quality assurance value greater than 0.5. In Table 1, we report information regarding the analysis results and temporal resolution of instruments and models used in the framework.

2.3.3. Mesoscale Atmospheric Modeling Products

To assess the prevailing circulation conditions during the study period we use the non-hydrostatic Weather Research and Forecasting model (WRF) [35] version 4.2. Two two-way nested domains are adopted, with horizontal grid spacing of 10 and 2 km respectively; the innermost higher resolution domain (281 × 296 horizontal grid points), covering Southern Italy, is considered adequate to resolve most mesoscale features in the orographically complex study area. The model is implemented with 40 terrain-following vertical levels more closely spaced in the boundary layer, 15 of them below 2000 m in height. Initial and boundary conditions are derived from the National Center for Environmental Prediction–Global Forecast System (NCEP–GFS) analyses/forecast (0.25-degree horizontal resolution), and the model configuration is derived by those operationally adopted by CNR-ISAC and borrowed by recent works regarding other wind-related extreme weather events in Italy [36,37].

In particular, the main physical parameterizations are the Asymmetrical Convective Model version 2 (ACM2) scheme for the planetary boundary layer, the new Rapid Radiative Transfer Model (RRTMG) long-wave and short-wave radiation scheme, the Noah land-

surface model, the Thompson microphysics scheme, and the Betts–Miller–Janjić (BMJ) cumulus parameterization; the latter is activated only for the coarse grid, while convection is explicitly resolved for the fine grid. A general description of the WRF physics options and references is available on the model's user page [38].

3. Results

Before delving into the discussion of the case study associated with fire events, we examine the correlation between meteorological parameters with trace gases (CO_2, CO) and eBC during summer seasons.

A bivariate statistical analysis is used to provide useful hints meant to investigate the influence of local wind regimes to the observed atmospheric species.

To this aim, for the summer seasons from 2017 to 2021, hourly mean values of eBC, CO and CO_2 are analyzed as a function of wind speed and direction observed at LMT (Figure 2). The highest values of eBC concentrations (>0.55 µg/m^3), and trace gases (CO > 110 ppb, CO_2 > 410 ppm) are observed for winds coming from the east-northeast (Figure 2). This implies a role of air masses from inland in favoring the occurrence of elevated values of these atmospheric tracers, under local circulation (mountain breeze, with wind velocity < 5 m/s). The data characterized by lower values observed for this air-mass provenance are associated to a cyclonic event characterized by higher wind speed. When we consider the west and southwest (W-SW) sectors, two different situations generally occur: one related to the establishment of the breeze regime, with winds lower than 6 m/s and characterized by the transport of marine aerosol; the other related to synoptic conditions with winds stronger than 8 m/s characterized by the transport of Saharan-type aerosols or ash coming from the nearby volcanoes Etna (2 km as the crow flies from the observatory, 3357 m *above ground level*) and Stromboli (1 km as the crow flies from the observatory, 924 m *above ground level*) in front of the coastline [28]. The first occurrence was the most frequent at LMT during the summer season; therefore, the concentrations of eBC, CO and CO_2 in the W–SW sectors were lower than 0.8 µg/m^3, 80 ppb and 410 ppm, respectively. In the west sector, the eBC, CO and CO_2 concentrations decreased considerably down to 0.2 µg/m^3, 30 ppb and 400 ppm, respectively, agreeing to the advection of the sea air masses (>8 m/s). This decrease was also evident for the northwest sectors. With respect to the south south-east sectors, eBC concentration > 2 µg/m^3, CO > 150 ppb and CO_2 > 440 ppm were observed and related to the open fire events.

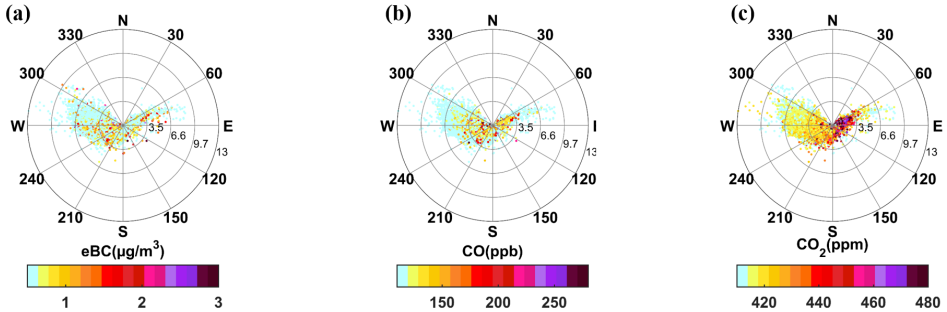

Figure 2. Bivariate analyses: hourly mean values of eBC (**a**), CO (**b**) and CO_2 (**c**) as a function of wind speed and direction for summer 2017–2021.

In Figure 3, we report a standard statistical analysis in order to analyze the interannual variability of the observed values of temperature, eBC, CO and CO_2. In detail, based on the hourly mean values of the considered variables, we calculate the seasonal mean, median values as well as the 5th, 25th, 75th and 95th percentiles. Moreover, for each single year, we calculate the monthly mean values related to August. The highest monthly averaged value of air temperature (27.0 ± 0.3 °C, mean value ± 1 sigma) over the period 2017–2021 is observed in August 2021 (Figure 3a). In the same month, we recorded the following averaged concentrations: eBC (Figure 3b) 0.74 ± 0.36 µg/m^3, CO (Figure 3c) 147 ± 48 ppb

and CO_2 (Figure 3d) 435 ± 24 ppm. For each single year in 2017–2021, the highest monthly temperature, eBC and CO were all related to August, with lower values observed in the remaining months (June and July). Based on this evidence, we decided to focus on August months to investigate the possibility that open fires in the region may have influenced the atmospheric composition variability at LMT.

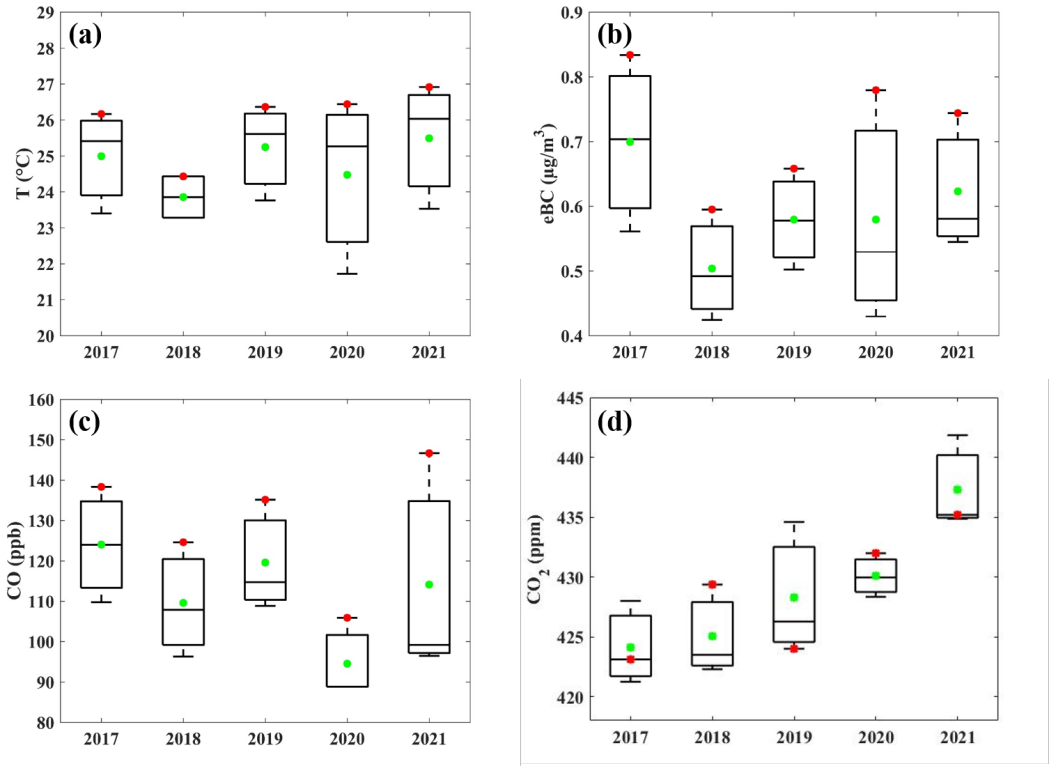

Figure 3. For each year between 2017 and 2021, we report the average summer season values (green spots), the mean values for August months (red spots), the median (bold lines) and the 5th, 25th, 75th and 95th percentiles (box and whiskers) for air temperature (**a**), eBC (**b**), CO (**c**) and CO_2 (**d**).

Given the evidence of high concentrations of the parameters in the months of August, we analyzed the fire events in the area under study. In Figure 4, we show the number of daily active fires during the months of August between, 2017 and 2021, detected by the MODIS satellite in the "focus" area (orange box in Figure 1). It is interesting to note that in August 2021, MODIS detected a significant peak in fire number (i.e., 42) between 8 and 12 August, representing the record of fire activity since 2017. Note that the number of fires are reported as the original GFED4 data without taking into account the transport time to the observatory. Considering what was observed by the satellite data, we focused our attention on the time window between 8 and 12 August 2021.

With the purpose of pointing out the possible signals of the open fire emissions to the atmospheric tracers observed at LMT, we considered the continuous time series of wind direction, eBC, CO and CO_2 from 5 to 15 August 2021 (Figure 5). To support the analysis of surface data, we used satellite data (columnar measurements by satellite) and a regional-scale weather model. By adopting this approach, we were able to detect, on a local scale, the effects of fire events recorded near the experimental site. CO total column satellite products were determined from the selected Level-2 TROPOMI Offline data, while the reprocessing stream and the analysis of the CO column were performed through an algorithm developed in MatLab-R2016a with a number of consecutive digital processing steps. In Figure 6, we report the daily comparison between CO at the surface expressed as ppb and CO total column satellite (molecules/m^2) concentrations at 01:00 p.m. UTC over the period 5–15 August 2021.

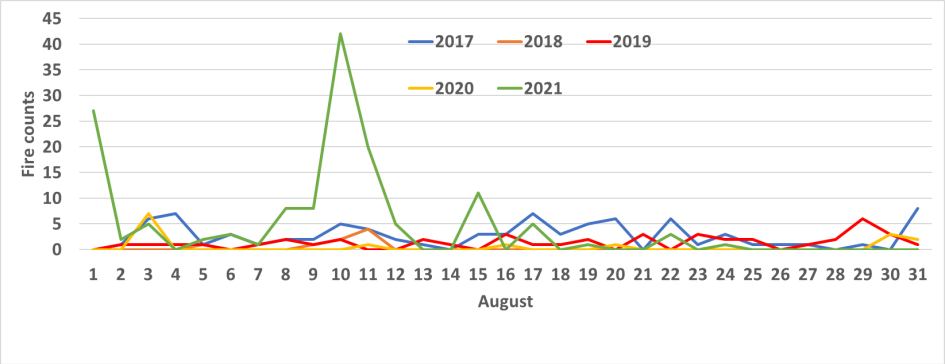

Figure 4. Time series reporting the number of August daily active fires detected by GFED4 (MODIS satellite) in the study area (see Figure 1) for years 2017–2021. The y-axis shows the number of fires in the selected area.

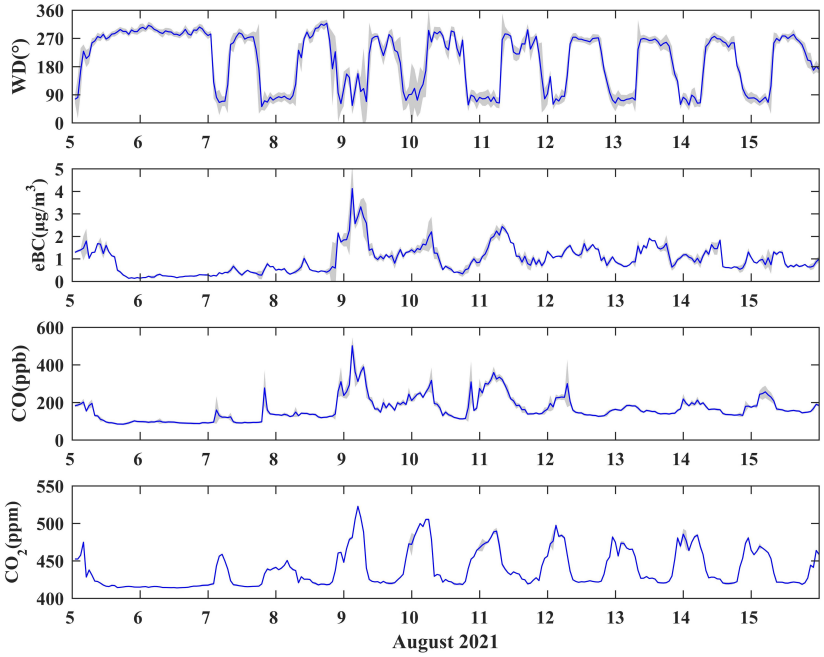

Figure 5. The time series of hourly mean values with respective standard deviations (grey shadow) for the period from 5 to 15 August 2021 for wind direction, concentrations of eBC, CO, and CO_2 observed at LMT.

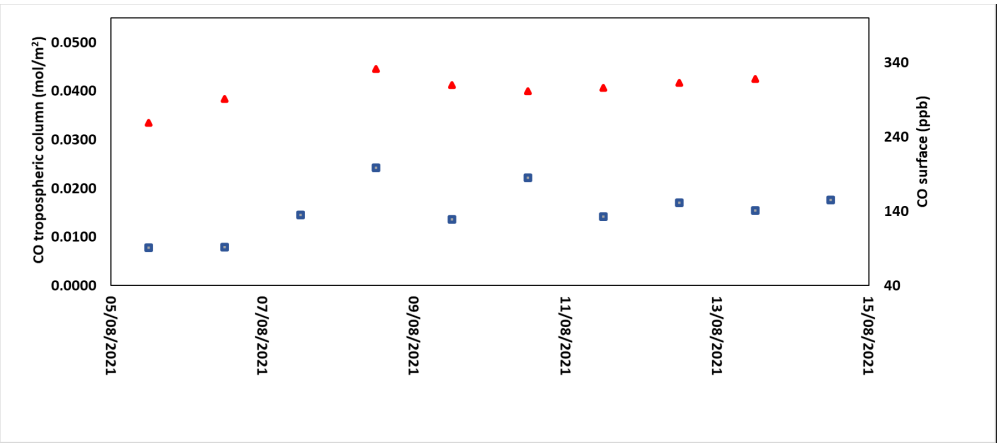

Figure 6. Comparison between near-surface CO values (blue squares) at LMT observed at 01:00 p.m. UTC and tropospheric column in molecules/m^2 (red triangles) by TROPOMI L2 product. The considered period ranges from 5 to 15 August 2021.

4. Discussion

Our work documents the potential contributions to the study of open burning emissions resulting from the integration of experimental, satellite and modeling data in the Calabria region. In particular, here, we discuss the possibility that open fires occurring in August 2021 affected the atmospheric composition observed at the LMT WMO/GAW station. To better investigate the possible relationship between the identified fire events and the atmospheric composition variability at LMT, we inspected the time series of fire emission tracers (CO_2, CO and eBC) together with wind speed and direction (Figure 5). eBC concentration values started to increase at 09:00 p.m. on 8 August, reaching the maximum value of 4.12 ± 0.02 µg/m^3 at 02:00 a.m. on the 9 August; higher values than the seasonal summer 2021 mean of 0.6 ± 0.2 µg/m^3 were recorded in the following days until the 11th of the same month, with further maximums of 2.22 ± 0.02 µg/m^3 on the 10 August at 06:00 a.m. and 2.43 ± 0.02 on the 11 August at 07:00 a.m. During these days, a similar temporal variability is observed for CO_2 and CO, with reported maximums of 502.0 ± 44.1 ppb, 317.6 ± 68.1 ppb, 359.2 ± 30.8 ppb of CO and 522.8 ± 0.2 ppm, 505.3 ± 1.3 ppm, 489.7 ± 4.4 ppm of CO_2, on 9 August at 02:00 a.m., on 10 August at 06:00 a.m. and on 11 August at 04:00 a.m., respectively. Correspondingly regarding the increases in concentration relating to all parameters, the origin of the air masses from the south and south-east quadrants was highlighted, which began on 8 August at 07:00 p.m. and persisted until 07:00 a.m. the next day. In the days that followed, the wind regimes were established so that during the nighttime hours, air masses continued to arrive from the eastern sector, carrying plumes of smoke with them. Among the particulate combustion products, in addition to the eBC, it is also interesting to observe the values of atmospheric particulates of different sizes.

The analysis is therefore focused also on the cumulative daily concentrations of $PM_{2.5}$ and PM_{10} of August 2021. On the 9th, $PM_{2.5}$ recorded its maximum value of 15.2 ± 0.5 µg/m^3 by sampling the products due to fire event-related combustion processes. The concentration contribution relative to PM_{10} sampling was also significant, i.e., 27.7 ± 0.5 µg/m^3. During the days of fire events, the concentrations values of $PM_{2.5}$ and PM_{10} on the 11th were 14.2 ± 0.5 µg/m^3, 36.9 ± 0.5 µg/m^3 and 12th 26.4 ± 0.5 µg/m^3, 10.7 ± 0.5 µg/m^3 respectively. The latter were higher during these events, with the monthly mean of August with respect to PM_{10}, 22.5 ± 0.5 µg/m^3, and $PM_{2.5}$, 9.9 ± 0.5 µg/m^3. The increase in these two fractions of atmospheric particulates indicates the presence of combustion processes detected at the experimental site.

The air masses transport over Calabria was studied by a mathematical model (WRF) and the wind conditions of the whole period of interest were simulated.

Synoptic features were analyzed using the NCEP-GFS data (0.25-degree horizontal resolution), the same as those adopted for the WRF initial and boundary conditions. The analysis revealed (related maps are reported in Figure 7) a stationary synoptic configuration for the whole period, with general atmospheric stability conditions. On 8 August, a wide upper-level (500 hPa) ridge dominated the whole Mediterranean Basin, with a high pressure area between Northern Africa and Southern Italy (upper panels of Figure 7). This configuration persisted for the whole period, only slowly moving westward in the next days (the upper-level high-pressure area was in fact located over the Strait of Gibraltar on 13 August as shown in Figure 7). Zonal upper-level flows approached the Mediterranean and a cyclonic circulation affected Southern Italy. At the surface, a leveled-pressure regime prevailed, with weak winds with cyclonic rotation over Southern Italy, predominantly from the south over the central areas of Calabria (bottom panels of Figure 7). To better assess the local circulation over the study area, we report in Figure 8 the 10 m wind speed and direction (vectors) simulated by the high-resolution (2 km) WRF model in the initial phases of fire events, in particular immediately before (08:00 p.m. UTC on 8 August) and after (11:00 p.m. UTC on 8 August) the increase in all parameters described in Figure 5 in LMT.

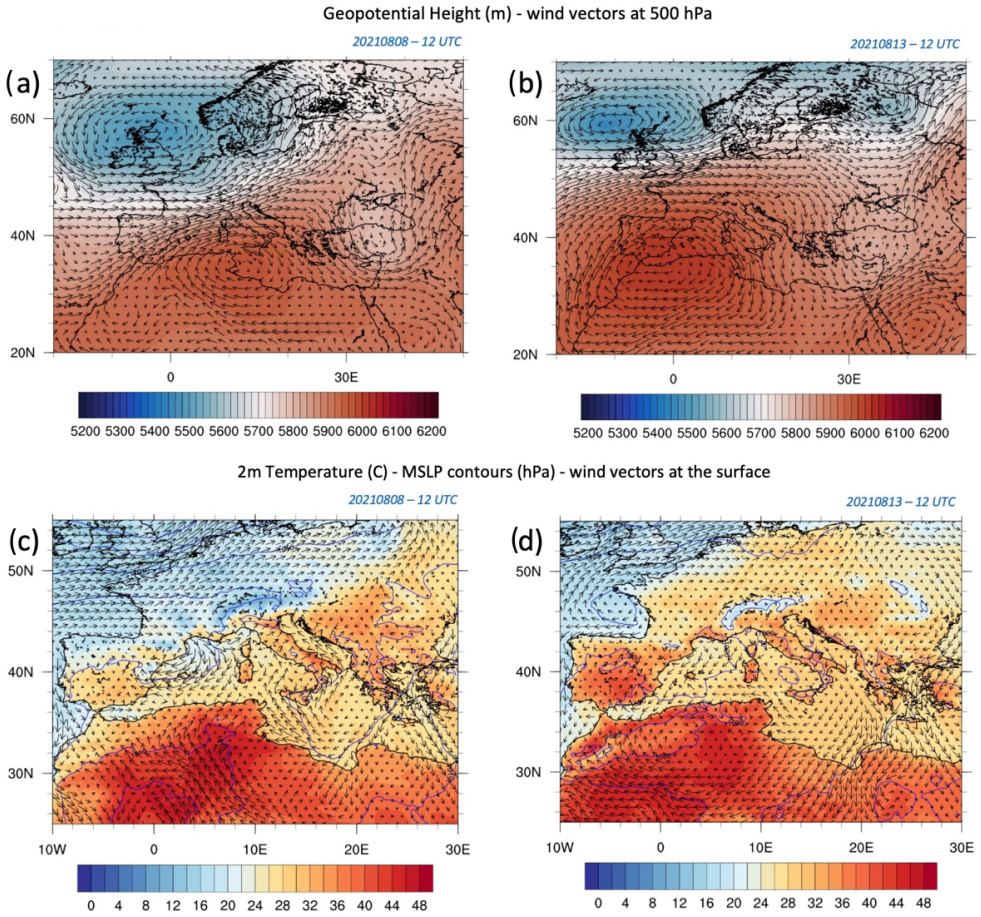

Figure 7. NCEP-GFS Geopotential Height (m) and wind vectors at 500 hPa, for 8 August 2021 at 12:00 a.m. UTC (**a**) and 13 August 2021 at 12:00 a.m. UTC (**b**). NCEP-GFS 2 m temperature (°C), Mean Sea Level Pressure, MSLP (hPa) and wind vectors at the surface for 8 August 2021 at 12:00 a.m. UTC (**c**) and 13 August 2021 at 12:00 a.m. UTC (**d**).

To discuss the possibility that the fire plumes may have affected the atmospheric composition of a wide tropospheric layer, we analyzed the data from the COPERNICUS SP5 satellite to evaluate the presence of CO in the atmospheric column above the observatory. In Figure 6, the near-surface data recorded at 01:00 p.m. UTC (i.e., at the time of the TROPOMI passage) and the columnar data are compared. The comparison between the near-surface measurements at LMT and satellite datasets reveals a similar variability with a CO peak when fire events occurred. The analysis of the time series reported in Figure 5 shows the concentration decreases in eBC, CO_2 and CO at the surface. In the same period, CO concentrations comparable to 12 August (0.04 mol/m^2) are observed on the atmospheric column (Figure 6). This latter evidence is linked both to the lifetime of CO in the atmosphere [39] and to the speed of air masses and indicates the end of fire events.

The presence of south-south-easterlies winds affecting the LMT observatory, and the main fire locations (south-southeast from the observatory; see Section 3), support the hypothesis by which the recorded eBC, CO, CO_2, PM_{10}, and $PM_{2.5}$ concentration peaks during the case study could be directly connected to the wind-driven transport of combustion products from the locations where fires took place. The directionality of the atmospheric circulation and wind fields with respect to the location of the experimental site were able to provide sufficient information to corroborate the hypotheses of comparison between the sources of fire events and the concentrations of the combustion products detected by satellite and in situ data. In this regard, the occurrence of fire events on the southeastern side of the Aspromonte Massif in Calabria was identified by satellite data

as sketched in Figure 9a but not detected by our instruments since the wind fields move longitudinally to the east coast line as shown in Figure 9b.

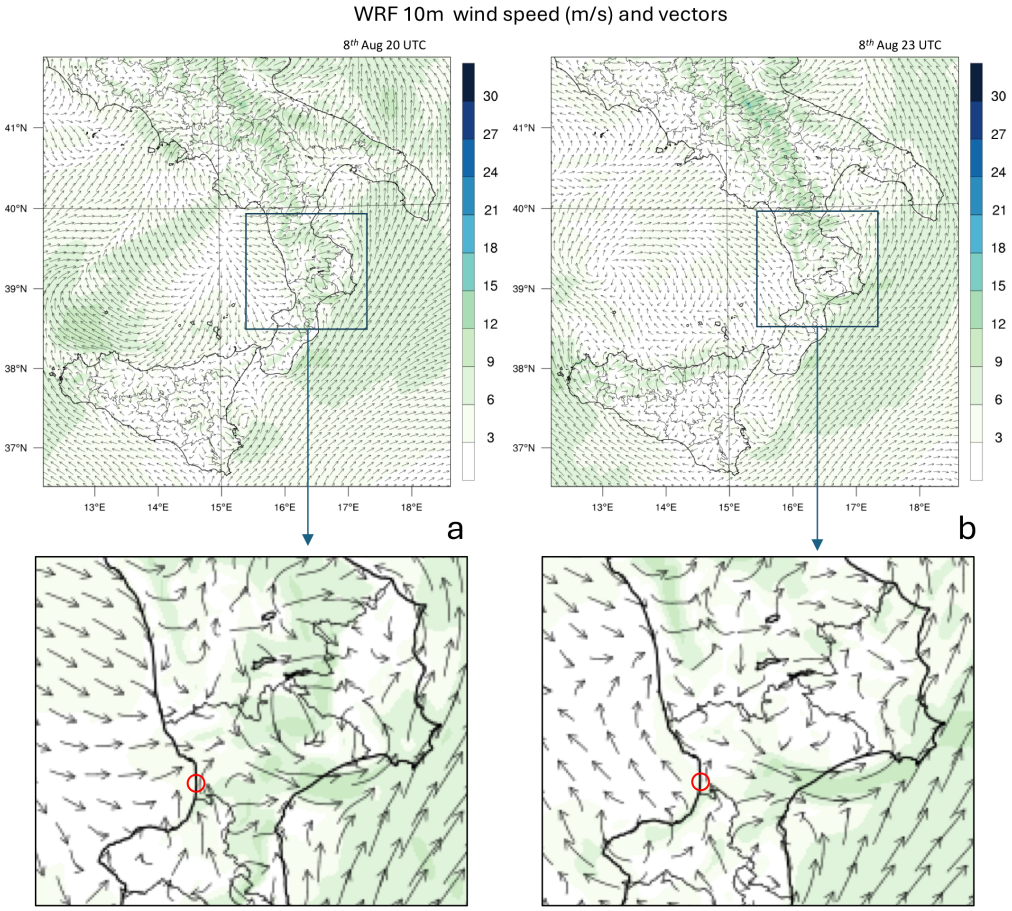

Figure 8. WRF (2 km resolution) 10 m wind speed (m/s) and wind vectors, for 8 August 2021 at 08:00 p.m. UTC (**a**) and 11:00 p.m. UTC (**b**); the red circle approximately indicates the LMT observatory.

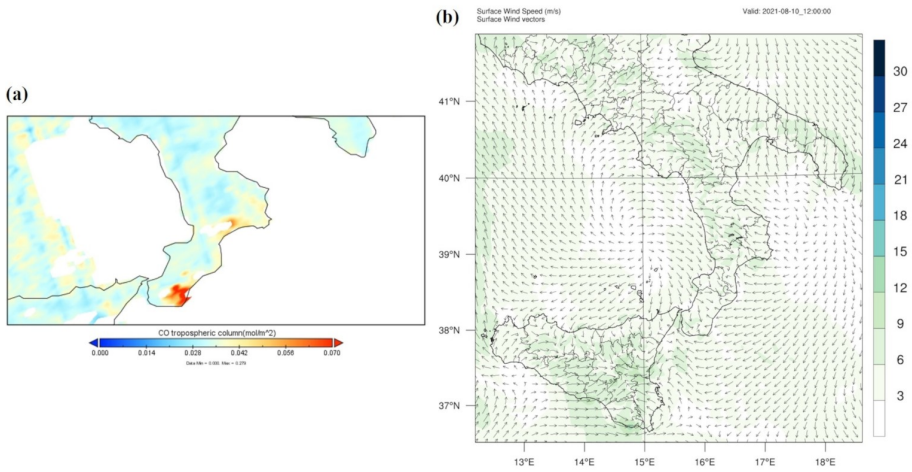

Figure 9. Identification of fires occurrence at Aspromonte Massif site via CO concentration by using satellite data (**a**) and wind circulation (**b**) from WRF output map on 10 August 2021.

5. Conclusions

Over the past last years, several exceptional wildfires have occurred across the globe, overwhelming suppression capabilities, causing substantial damage, and often resulting

in fatalities. Fire events play an important role as contributors in the concentrations of gases and aerosols in the atmosphere. The repeatability and severity of such events is increasing the amount of the combustion products. The originality of this paper lies in the attempt to develop an integrated approach to analyze the impact of fire events to the atmospheric composition in Calabria, Southern Italy (Mediterranean basin). A methodology was implemented to discriminate and identify the emission sources of fire events that we recorded at the permanent World Meteorological Organization (WMO) of Global Atmosphere Watch (GAW) observatory at Lamezia Terme (Code: LMT). A further aim of this work is to contribute to the knowledge of the impact of open fires on atmospheric composition variability. Despite the existence of plans for the prevention and management of fire events in Calabria, the work is useful to visualize not only natural damage but also short- and medium-range emissions. In particular, we calculated interannual variability, summer and monthly mean values of the summer seasons, 2017–2021. We investigated a case study of trace gases and particulate matter transport as combustion products from fire events. We registered a sevenfold increase in the maximum concentration value during the case study for eBC (4.12 $\mu g/m^3$), and a fourfold increase in CO (502.03 ppb) compared to the summer seasonal average 2021 of 0.62 $\mu g/m^3$ and 114.13 ppb, respectively. Furthermore, the maximum concentration value of CO_2 was 522.8 ppm, which is notably higher than the summer seasonal average 2021 of 437.3 ppm. eBC and CO appeared to be the most suitable tracers of fire events at the LMT site due to its peculiarities with respect to orography and local circulation. This work represents a valuable starting point to carry on a systematic long-term study over the entire available dataset. The framework would be extended and integrated to wider spatial scales (i.e., Southern Mediterranean area) on the basis of regional circulation that allows fire emission transport from medium and long ranges.

Author Contributions: Formal analysis, T.L.F.; Investigation, T.L.F., P.C. and C.R.C.; Data curation, L.M., D.P., T.L.F., P.C. and C.R.C.; Writing—original draft, L.M., D.P., T.L.F., E.A., P.C. and C.R.C.; Writing—review & editing, L.M., D.P., T.L.F., E.A., I.A., D.G., S.S., P.C., M.D.P., F.D. and C.R.C.; Supervision, C.R.C.; Project administration, M.D.P. All authors have read and agreed to the published version of the manuscript.

Funding: This work was developer under partially funded by Ministry of Research and University IR Project PRO-ICOS-MED CIR0019 (MUR-PON 2014-2020), and by IR0000032—ITINERIS, Italian Integrated Environmental Research Infrastructures System (D.D. n.130/2022—CUP B53C22002150006) Funded by EU—Next Generation EU PNRR- Mission 4 "Education and Research"—Component 2: "From research to business"—Investment 3.1: "Fund for the realisation of an integrated system of research and innovation infrastructures".

Data Availability Statement: Data are accessible, through CNR-ISAC data policy and registration at https://adc.isac.cnr.it/.

Conflicts of Interest: The authors declare no conflicts of interest.

References

1. Costa, H. European wildfire danger and vulnerability in a changing climate: Towards integrating risk dimensions. In *Technical Report by the Joint Research Centre: JRC PESETA IV Project: Task 9 Forest Fires*; Publications Office of the European Union: Luxembourg, 2020.
2. Bowman, D.M.J.S. Fire in the earth system. *Science* **2009**, *324*, 481–484. [CrossRef] [PubMed]
3. Keeley, J.E. Fire as an evolutionary pressure shaping plant traits. *Trends Plant Sci.* **2011**, *16*, 406–411. [CrossRef] [PubMed]
4. Pausas, J.G. A burning story: The role of fire in the history of life. *Bioscience* **2009**, *59*, 593–601. [CrossRef]
5. Lambers, H. *Plant Physiological Ecology*; Springer: Cham, Switzerland, 2008; Volume 2, pp. 4–6.
6. Ruffault, J. Increased likelihood of heat-induced large wildfires in the Mediterranean Basin. *Sci. Rep.* **2020**, *10*, 13790. [CrossRef] [PubMed]
7. Belcher, C.M. Baseline intrinsic flammability of Earth's ecosystems estimated from paleoatmospheric oxygen over the past 350 million years. *Proc. Natl. Acad. Sci. USA* **2010**, *107*, 22448–22453. [CrossRef] [PubMed]
8. Dupuy, J. Climate change impact on future wildfire danger and activity in southern Europe: A review. *Ann. Forest Sci.* **2020**, *77*, 35. [CrossRef]

9. Turco, M. Exacerbated fires in Mediterranean Europe due to anthropogenic warming projected with non-stationary climate-fire models. *Nat. Commun.* **2018**, *9*, 3821. [CrossRef] [PubMed]
10. Field, C.B. White, Climate Change 2014: Impacts, Adaptation and Vulnerability. Renewable and Sustainable Energy Reviews. 2014. Available online: https://www.ipcc.ch/report/ar5/wg2/ (accessed on 26 March 2024).
11. Singh, S. Forest fire emissions: A contribution to global climate change. *Front. For. Glob. Chang.* **2022**, *5*, 925480 . [CrossRef]
12. Andrea, M.O. Transport of biomass burning smoke to the upper troposphere by deep convection in the equatorial region. *Geophys. Res. Lett.* **2001**, *28*, 951–954. [CrossRef]
13. Andrea, M.O. Emission of trace gases and aerosols from biomass burning—An updated assessment. *Atmos. Chem. Phys.* **2019**, *19*, 8523–8546. [CrossRef]
14. Ribeiro-Kumara, C. How do forest fires affect soil greenhouse gas emissions in upland boreal forests? A review. *Environ. Res.* **2020**, *184*, 109328. [CrossRef] [PubMed]
15. Van der Werf, G.R. Global fire emissions estimates during 1997–2016. *Earth Syst. Sci. Data* **2017**, *9*, 697–720. [CrossRef]
16. Zheng, B. Increasing forest fire emissions despite the decline in global burned area. *Sci. Adv.* **2021**, *7*, eabh2646. [CrossRef] [PubMed]
17. Chatfield, R.B. Emissions relationships in western forest fire plumes—Part 1: Reducing the effect of mixing errors on emission factors. *Atmos. Meas. Tech.* **2020**, *13*, 7069–7096. [CrossRef]
18. Liang, Y. Emissions of organic compounds from western US wildfires and their near-fire transformations. *Atmos. Chem. Phys.* **2022**, *22*, 9877–9893. [CrossRef]
19. Akagi, S.K. Emission factors for open and domestic biomass burning for use in atmospheric models. *Atmos. Chem. Phys.* **2011**, *11*, 4039–4072. [CrossRef]
20. Algeri, A. The potential of agricultural residues for energy production in Calabria (Southern Italy). *Renew. Sustain. Energy Rev.* **2019**, *104*, 1–14. [CrossRef]
21. Available online: https://www.regione.calabria.it/website/portaltemplates/view/view_provvedimenti.cfm?63819 (accessed on 26 March 2024).
22. Available online: https://www.regione.calabria.it/website/portalmedia/decreti/2023-05/Piano-AIB-2023_CV_rev05.pdf (accessed on 26 March 2024).
23. Available online: https://www.regione.calabria.it/website/portalmedia/decreti/2024-05/PIANO-AIB-2024.pdf (accessed on 26 March 2024).
24. Rönkkö, T. Review of black carbon emission factors from different anthropogenic sources. *Environ. Res. Lett.* **2023**, *18*, 033004. [CrossRef]
25. Donateo, A. Long-term observations of aerosol optical properties at three GAW regional sites in the Central Mediterranean. *Atmos. Res.* **2020**, *241*, 104976. [CrossRef]
26. Cristofanelli, P. Significant variations of trace gas composition and aerosol properties at Mt. Cimone during air mass transport from North Africa—Contributions from wildfire emissions and mineral dust. *Atmos. Chem. Phys.* **2009**, *9*, 4603–4619. [CrossRef]
27. Schultz, M.G. The Global Atmosphere Watch reactive gases measurement network. *Elem. Sci. Anthr.* **2015**, *3*, 000067. [CrossRef]
28. Lo Feudo, T. Study of the vertical structure of the coastal boundary layer integrating surface measurements and ground-based remote sensing. *Sensors* **2020**, *20*, 6516. [CrossRef]
29. Calidonna, C.R. Five years of dust episodes at the Southern Italy GAW Regional Coastal Mediterranean Observatory: Multisensors and modeling analysis. *Atmosphere* **2020**, *11*, 456. [CrossRef]
30. Crotwell, A. *GAW Report N 255, Jeju Island, Republic of Korea*; World Meteorological Organization: Geneva, Switzerland, 2020.
31. Petzold, A. Multi-angle absorption photometry—A new method for the measurement of aerosol light absorption and atmospheric black carbon. *J. Aerosol Sci.* **2004**, *35*, 421–441. [CrossRef]
32. Randerson, J.T. *Global Fire Emissions Database*; Version 4, (GFEDv4); ORNL DAAC: Oak Ridge, TN, USA, 2018. [CrossRef]
33. Veefkind, J. TROPOMI on the ESA Sentinel-5 Precursor: A GMES mission for global observations of the atmospheric composition for climate, air quality and ozone layer applications. *Remote Sens. Environ.* **2012**, *120*, 70–83. [CrossRef]
34. European and Space and Agency, (ESA). Sentinel-5 Precursor/TROPOMI Level 2 Product User Manual Carbon Monoxide Document Number. 2021. Available online: https://sentinel.esa.int/documents/247904/2474726/Sentinel-5P-Level-2-Product-User-Manual-Carbon-Monoxide.pdf (accessed on 26 March 2024).
35. Skamarock, W.C. A Description of the Advanced Research WRF Version 4. NCAR Tech. Note NCAR/TN-556+STR. 2019; Volume 145. Available online: http://dx.doi.org/10.5065/1dfh-6p97 (accessed on 26 March 2024).
36. Avolio, E. Tornadoes in the Tyrrhenian regions of the Italian peninsula: The case study of 28 July 2019. *Atmos. Res.* **2022**, *278*, 106285. [CrossRef]
37. Avolio, E. Multiple tornadoes in the Italian Ionian regions: Observations, sensitivity tests and mesoscale analysis of convective storm environmental parameters. *Atmos. Res.* **2021**, *263*, 105800. [CrossRef]
38. Available online: https://www2.mmm.ucar.edu/wrf/users/physics/phys_references.html (accessed on 26 March 2024).
39. Khalil, M.A. Carbon Monoxide in the Earth's Atmosphere: Increasing Trend. *Science* **1984**, *224*, 54–56.